Influence of testing and tempering temperatures on fatigue behaviour, life and crack initiation mechanisms in a 5%Cr martensitic steel

Denis Delagnes, Farhad Rezai-Aria, Christophe Levaillant

Available online at www.sciencedirect.com
ScienceDirect
Procedia Engineering 2 (2010) 427–439
Procedia Engineering
www.elsevier.com/locate/procedia

Fatigue 2010

Influence of testing and tempering temperatures on fatigue behaviour, life and crack initiation mechanisms in a 5%Cr martensitic steel

D. Delagnes[a,b,*], F. Rézaï-Aria[a,b] and C. Levaillant[b]

a-Université de Toulouse ; INSA, UPS, Mines Albi, ISAE ; ICA (Institut Clément Ader); Campus Jarlard, F-81013 Albi cedex 09, France
b- Ecole des Mines Albi, Campus Jarlard, F-81013 Albi, France

Received 23 February 2010; revised 9 March 2010; accepted 15 March 2010

Abstract

The effects of temperature as well as the initial hardness in the range 42 to 50HRC on the fatigue behaviour and life of a 5%Cr tool steel are investigated. Total strain controlled isothermal fatigue experiments between 200°C and 600°C are carried out under 1Hz frequency. The significant softening induced by tempering and/or cyclic loading is related to a strong reduction of the dislocation density clearly observed by transmission electron microscopy and x-ray diffraction. The coalescence of secondary carbides is also involved in the yield strength decrease above 550°C and during cyclic loading. Increasing the initial hardness reduces the cyclic softening rate and increases the fatigue life. Moreover, several isothermal fatigue experiments with regular interruptions at different fractions of life are performed in order to investigate the crack initiation mechanisms. Three main crack initiation sites were observed depending on testing temperatures: non-metallic inclusions, prior austenitic grain boundary and lath boundary.

Keywords: martensitic tool steel; cyclic softening; dislocation structure, secondary carbides; crack initiation

1. Introduction

5% chromium steels were particularly developed for high temperature metal forming operations as pressure die casting for light alloys injection, forging dies, mandrels, extrusion tools, etc..[1]. High temperature tools are subjected to severe mechanical and thermal loads during hot operations. Indeed, the life of such tools is limited and ranges between few hundred to few 10^5 cycles or more respectively in hot forging or extrusion and high pressure die casting. At each production cycle, the tool is subjected to transient thermo-mechanical loads due to the contact between the material to be formed at high temperature and the tool surface working at lower temperature.

Mechanical properties of such martensitic steels are strongly connected to their complex microstructure obtained after heat treatment that are generally performed in order to achieve a good hardness and/or tensile strength with

* Corresponding author. Tel.: +33 5 63 49 32 48.
E-mail address: denis.delagnes@enstimac.fr

1877-7058
doi:10.1016/j.proeng.2010.03.047

sufficient ductility. As the high temperature fatigue is one of a general dominant damaging mechanism limiting the tool life, a systematic investigation of fatigue behaviour and life of a widely used 5% Cr steel within the AISI H11 family was undertaken. Influence of temperature and initial hardness on fatigue behaviour and life are examined in order to understand the mechanisms associated to the limited life of these tools [2] in a quite large number of cycles to failure range.

However, it is of great importance to clearly understand the microstructural mechanisms controlling fatigue properties and probably due to experimental difficulties, microstructural parameters (such as carbides at a nanometric scale and dislocations) giving suitable usual mechanical properties are therefore scarcely fully investigated. Notably, martensitic or bainitic steels have a typical fatigue behaviour as these steels present a strong softening till rupture (of about 25% of the stress amplitude measured during the first cycle for the AISI H11 steel, see Fig.1 [2,3]).

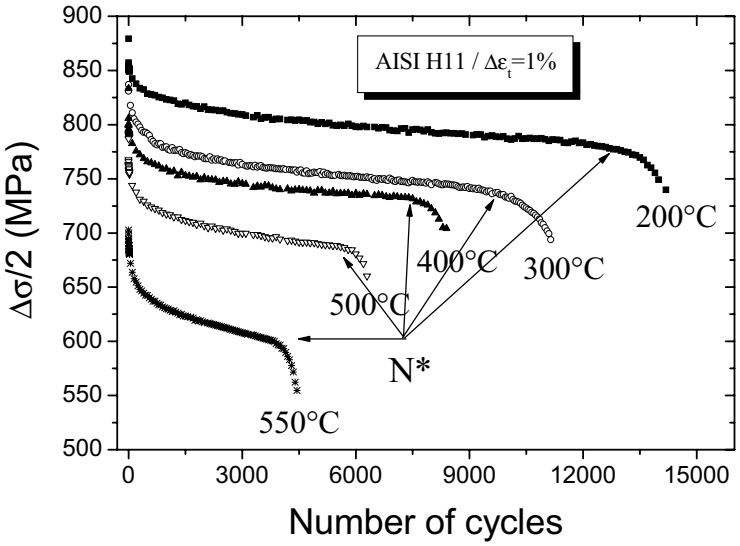

Fig. 1. Temperature influence on cyclic behaviour of the AISI H11 steel.

This cyclic softening is unfortunately not taken into account during the steelmaking process or the optimisation of tool design through numerical finite elements. Such calculations of stress and strain fields require constitutive models able to describe accurately the macroscopic behaviour [4,5]. Moreover the cyclic softening can be linked to both microstructural evolution and crack propagation (inducing a loss of force amplitude while the resistant area is decreasing for strain control experiments). To investigate which effect is prevailing, several fatigue tests were regularly interrupted and the replica technique allowing to detect the crack initiation was used. In addition, the major part of fatigue specimen were observed after rupture to investigate the main crack initiation sites according to the testing temperatures. The steel investigated and experimental details are presented in the second part. Results dealing with the influence of tempering temperatures and fatigue loading on the cyclic behaviour, fatigue life and main crack initiation mechanisms are presented and discussed in the third part.

2. Experimental procedure

The composition of the modified AISI H11 (low Silicon content) grade investigated is shown in Table 1. Heat treatment includes austenitizing for one hour followed by air cooling, first tempering at 550°C for two hours, second tempering for two hours between 550°C and 640°C depending on desired hardness.

Table 1 : Mod. AISI H11 chemical composition (weight %)

	C	Cr	Mo	V	Si	Mn	P	Sn	Sb
Weight %	0,36	5,06	1,25	0,49	0,35	0,36	0,006	0,0022	0,0005

The table 2 shows references and heat treatments of analysed samples :

Table 2 : Samples investigated

Reference	Heat treatment conditions	Fatigue test	Experimental yield strength ($\sigma_{y0.2}$) at room temperature (MPa) or cyclic softening amplitude
A1	Annealed	--	--
A2	As air quenched	--	--
A3	Tempered 550°C	--	1550
A4	Tempered 550°C + 580°C	--	1450
A5	Tempered 550°C + 600°C	--	1360
A6	Tempered 550°C + 620°C	--	1120
A7	Tempered 550°C + 640°C	--	950
A8	Same as reference A6	$\Delta\varepsilon_t$ = 1,5% at 550°C	Softening amplitude : 230MPa
A9	Same as reference A6	$\Delta\varepsilon_t$ = 2,0% at 550°C	Softening amplitude : 250MPa

Microstructures were investigated by TEM. Observations were performed on a JEOL 2010 and a Philips CM12 microscopes, the last one is equipped with an energy dispersive x-ray analysis (EDX). Carbides were extracted from the martensitic matrix using the well-known replica technique. Diffraction in the selected area mode and EDX have been performed in order to determine carbides chemical composition and crystal structure whereas dislocations structure were examined on thin foils prepared by classical electropolishing.

X-ray diffraction experiments on the bulky material were also performed with peak profiles measurements in order to evaluate dislocation densities using the modified Williamson-Hall and the modified Warren-Averbach analysis [6,7].The diffraction peak profiles were both measured in the Eötvos University of Budapest with a special high resolution double-crystal diffractometer with negligible instrumental peak broadening [6,8] and in the CROMeP center using a PHILIPS X'PERT PRO diffractometer.

Isothermal total strain controlled fatigue tests were carried out on a servohydraulic testing machine equipped with a resistance furnace. Tests were performed at 200°C, 300°C, 400°C, 500°C, 550°C, 600°C with a total strain amplitude between 0,6% and 1,8%. The specimen final polishing was performed with a 1µm diamond suspension.

The axial strain was controlled and measured with a 10mm gauge length extensometer. The waveform of the cycle was triangular at a frequency of 1Hz, the mean strain being zero. Two samples (first tempering : 550°C 2h and second tempering : 620°C 2h) were selected to study the influence of fatigue on the evolution of carbides and dislocations. Fatigue tests were performed at 550°C which is an assumed temperature reached near the surface of the tool during high pressure die casting operations [9]. The two specimens were respectively cycled with a total strain amplitude of 1,5% and 2%.

3. Results and discussion

3.1. Fatigue behaviour

Figure 1 shows the half stress amplitude according to the number of cycles to failure for a total strain amplitude of 1%. For all the temperatures investigated, a continuous cyclic softening (stress amplitude decrease and plastic strain increase) till rupture is observed. The curves can be divided into 3 parts :

- A strong softening stage concentrated on the first hundreds cycles
- A linear softening stage which is observed during the major part of the life
- A sharp decrease of the stress amplitude due to propagation of one or several cracks in the specimen gauge length

This particular cyclic behaviour is typical of martensitic or bainitic steels. Indeed, softening is strongly associated to dislocations structure and density evolutions as well as to carbides nature, morphology and size modifications during cycling . Total softening amplitude, called D, was defined by the following equation :

$$D = \left(\frac{\Delta\sigma}{2}\right)_{N=1} - \left(\frac{\Delta\sigma}{2}\right)_{N=N^*} \quad (1)$$

where N* is the number of cycles to failure (see figure 1). At N*, the measured crack depth is around 200µm [2] in every cases.

At 300°C, the total softening amplitude reaches 170MPa representing nearly 20% of the stress amplitude measured at the first cycle (cf figure 2). Consequently, this strong softening effect should be taken into account to obtain a reasonable stress distribution of in-service tool and it is also necessary to look for a realistic cyclic behaviour law that should be implemented in finite elements calculation code. These results also show that doing a correlation between the hardness levels measured on a damaged tool and a service temperature is not relevant because the softening may not be due to an overheating if the tool was cycled over the « true » yield stress. So, martensitic or bainitic steels exhibit a continuous softening from the first cycle till rupture; this is a typical fatigue behaviour more complex to understand and to model than the major part of the metallic materials investigated which stabilise after a few tens or hundreds of cycles. As it was already reported by different authors, the cyclic softening is first explained by a strong decrease of the high dislocation density generated during the quench and a subsequent modification of the dislocation structure [2-4,10-18]. First, the tangle of dislocations is gradually crushed and dislocation cells are formed after several cycles. Dislocation density becomes very heterogeneous with a strongly reduced density inside the cells. Such a configuration promotes free motion of the dislocations between the walls, and free slip distances are increased. However, dislocation cell formation is not the single mechanism. Indeed, a second mechanism inducing softening is observed in very thin martensitic laths where the annihilation of dislocations occurs by cross-slip of screw dislocations and the climb of edge dislocations at high temperatures. Thus, a strong reduction of dislocation density is observed without any cell formation. The third mechanism involved in the softening is the growth and coalescence of secondary carbides [19-21] which also modifies the free slip distances of dislocations. This mechanism is obviously thermally activated and moreover, the secondary carbides coalescence is clearly accelerated under fatigue at elevated temperature [2,3]. Such dynamic ageing has already been observed in tempered martensitic steels, particularly under long-term creep conditions [22-24]. Moreover, the morphology of very elongated platelets, probably due to a crystallographic coherence with the matrix, is gradually

lost to achieve a more globular shape. These mechanisms also contribute to cyclic softening promoting dislocation mobility and reducing the steel resistance due to the fine precipitation occurring during tempering. To investigate if the softening can also be observed and estimated by hardness measurements, some fatigue specimen were selected at each testing temperatures. Considering the fact that softening is mainly induced by plastic strain, the adopted criterion of selection is as follows: hardness tests were performed on fatigue specimen presenting a plastic strain amplitude measured at half life of nearly 0.1%. Thirty indentations were performed using a Buehler® MICROMET® microhardness tester. The difference between hardness levels measured before the test and after as well as standard deviations are indicated in Table 3.

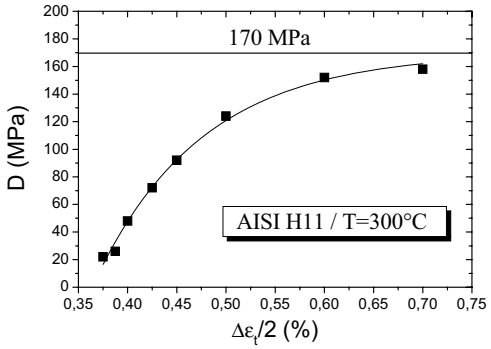

Fig. 2. Softening amplitude according to the total strain amplitude

Table 3 : Comparison between softening amplitudes and difference of microhardness.

Testing temperature (°C)	Hardness variation (Vickers : Hv) and corresponding standard deviation.	Softening amplitude (MPa)
200	5 (10)	140
300	0 (10)	125
400	20 (10)	130
500	45 (10)	110
550	65 (20)	90
600	80 (20)	160

At low temperatures (< ≈ 400°C), TEM observations have shown that the coalescence is obviously not observed after a fatigue test [2]. Taking into account the above-mentioned considerations, only the sharp decrease of the dislocation density is observed inducing an intense cyclic softening. However, this mechanism can not be revealed by hardness measurements, as a strong density of dislocations is introduced again during the indentation test. Therefore, the hardness level is only slightly modified at low temperatures as indicated in table 3.

Above 400°C, cyclic softening results from both reduction of dislocation density and coalescence of carbides [24]. As, the coalescence of carbides is not modified by the hardness measurement performed at room temperature, the cyclic softening can be partially detected. However, this test cannot describe the microstructural evolution when the rearrangement of dislocations generated by the quench is the main softening mechanism, which is obviously the case at low temperatures.

Nucleation, growth and coalescence of secondary carbides in the low silicon steel using both TEM observations and Small-Angle Neutron Scattering (SANS) were carefully described in previous works. Conversely, the dislocation density decrease during tempering or during cyclic testing is not so frequently investigated. Low magnification bright-field transmission electron image of sample A4 is shown in Fig. 3. Laths are clearly separated by elongated iron carbides. In addition, observations of thin foils show a high density of intralath entangled dislocations even for high tempering temperatures. Consequently, the identification of individual dislocations (Burgers vector and glide plane) and density evaluation is very difficult using the classical TEM technique. Prior to fatigue testing, dislocation distribution is quite homogeneous on the whole even if, at a nanometric scale, a high density of dislocations was observed both near lath boundaries and carbides. To qualitatively compare dislocation structures obtained at different tempering temperatures, observations were performed in the same crystallographic orientation conditions $\vec{g} = [\bar{1}\,10]$. The recovery of the microstructure is shown by the clear decrease of the dislocation density as the second tempering temperature increases. This effect is strongly increased by the application of a cyclic strain (see Fig. 4).

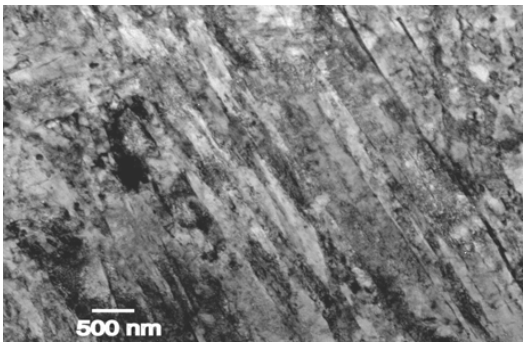

Fig. 3. Bright-field TEM image of the dislocation structure for the sample A4.

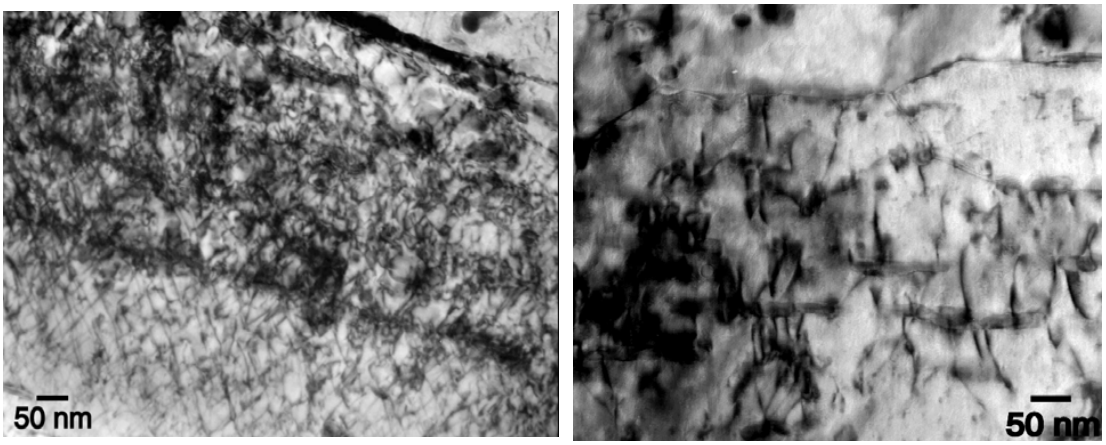

Fig. 4. Bright-field TEM images of the dislocation structure, $\vec{g} = [\bar{1}\,10]$. (a) before a fatigue test, sample A6, (b) after a fatigue test, sample A9 ($\Delta\varepsilon_t$ = 2.0%).

Coherently diffracting domains (CDD) and density of dislocations were evaluated using the theory and procedures introduced and developed by T.Ungár et al. [6-8,25,26]. Examples of conventional and modified Williamson-Hall plots are presented in Ref. [28]. The influence of the tempering temperature on CDD and density of dislocations are shown in Fig. 5. The highest density is measured for the as quenched sample (A2) in agreement with TEM observations. An increase of the second tempering temperature results in a strong decrease of the density of dislocations also in agreement with TEM observations previously described. Density decreases by a factor 20, between the as quenched sample and the specimen tempered at 640°C (A7). As dislocations contribute to limit the CDD size, the annihilation of dislocations results in an increase of CDD average size. As the consequence, the CDD size drastically increases with the temperature of the second tempering.

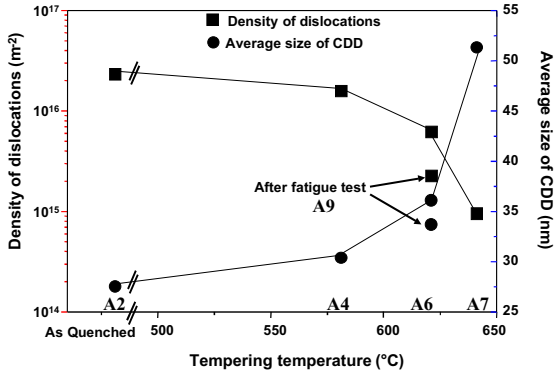

Fig. 5. Influences of tempering temperature and fatigue on the average size of CDD and the density of dislocations.

The influence of fatigue loading is also shown in Fig. 5 for a specimen tempered at 620°C (A6). After the fatigue test (A9), a decrease of the density of dislocations is observed. Conversely, no significant variation of CDD size occurs. The density of dislocations after fatigue is however higher than that estimated for the sample A7. This latter result seems to be inconsistent with TEM observations. TEM observations led to the conclusion that the fatigue effect seems to be qualitatively stronger than the effect of an increase of the tempering temperature. Indeed, fatigue loading induces a new arrangement of dislocations increasing the heterogeneity inside martensitic laths rather than a strong decrease of the density of dislocations.

Cyclic softening takes place for all the investigated temperatures (see figure 1). At 600°C, we observed a softening amplitude increase probably due to a modification of carbide sizes or chemical compositions at that temperature very close to the second tempering one.

As far as the initial hardness is concerned, a decrease of the total softening amplitude has been observed (see figure 6) for a constant total or plastic strain amplitude. The microstructure and so the macroscopic resistance of the steel tends to become more stable when the hardness level is increased. The better cyclic stability may be associated to a higher dislocations and carbides density that decrease dislocations mobility

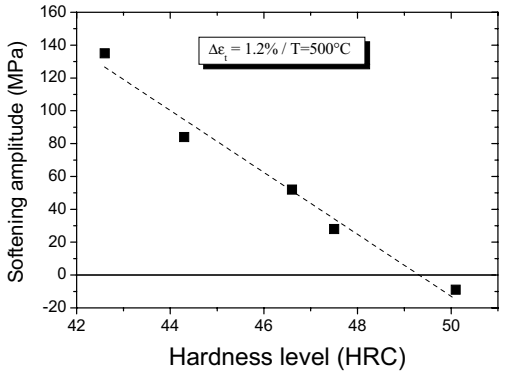

Fig.6. Hardness influence on the total softening amplitude for a fixed total strain amplitude

3.2. Fatigue life

Both Manson-Coffin and Basquin curves can well rationalised the fatigue life. Indeed, a life scattering factors equal to 2 were found for the Manson-Coffin law and 1.5 for the Basquin law [2] :

$$\frac{\Delta\varepsilon_p}{2} = \varepsilon'_f \left(2N^*\right)^c \quad Manson - Coffin \tag{2}$$

$$\frac{\Delta\sigma}{2} = C\left(N^*\right)^p \quad Basquin \tag{3}$$

where ε'_f is the fatigue ductility coefficient, c is the fatigue ductility exponent, C and p are the Basquin coefficient and exponent. Plastic strain and stress amplitudes are collected at half life (N*/2).

Initial hardness influence on life has been determined in the temperature range 300°C-600°C and the hardness range 42HRC-50HRC. When results are plotted in a Manson-Coffin diagram increasing the temperature till 550°C or increasing the hardness do not drastically modify Manson-Coffin curves taking into account life scattering. Resistance to cyclic plastic strain is not strongly affected even if a slight life reduction can be observed for hardness levels greater than 47HRC. When results are plotted in a Basquin diagram, influence of temperature is more evident. Increasing temperature leads to a strong life reduction. This influence becomes more pronounced between 500°C and 600°C where life reduction may reach a factor of 200 (see figure 7). Increasing hardness levels also has a strong effect on life (see figure 8). Till 550°C, Basquin exponent (p) values do not vary so much with the hardness level. These slight variations (around 20%) have been neglected and Basquin curves are considered to be parallel in a bi-logarithmic diagram. A life ratio for 2 different hardness levels, called F has been introduced :

$$F = \frac{N^*_{HRC2}}{N^*_{HRC1}} = \left(\frac{C_{HRC1}}{C_{HRC2}}\right)^{\frac{1}{p}} \tag{4}$$

Variations of F in function of hardness is presented on figure 9 at 500°C and 550°C. HRC1 is the hardness level of our reference state : 42HRC. For an equivalent stress amplitude, the life ratio can reach a value close to 1000 for a 8HRC increase at 500°C! Considering the fact that hardness are generally obtained after tempering with a scattering of 1HRC or 2HRC, it leads to a factor 2 to 5 for life scattering.

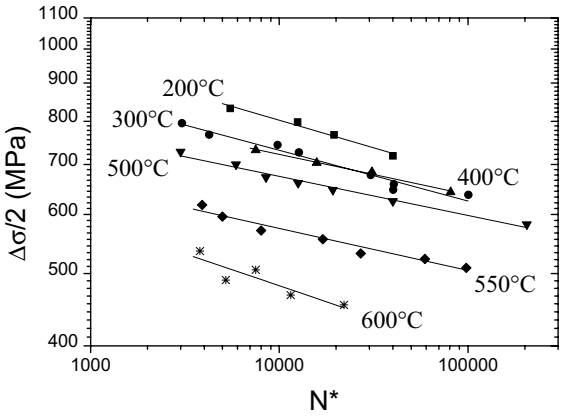

Fig. 7. Temperature influence on fatigue life in a Basquin diagram

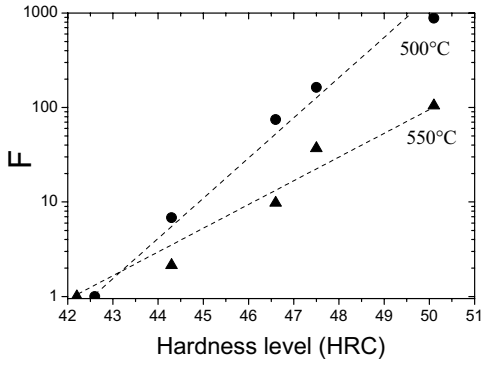

Fig. 8. Hardness influence on fatigue life

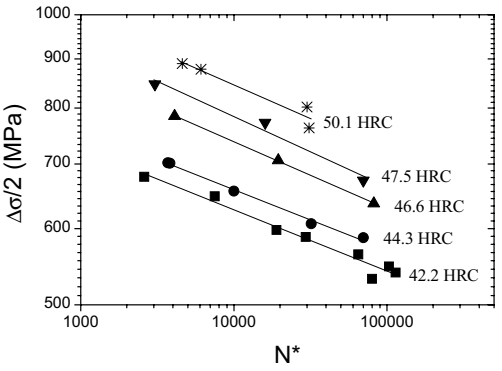

Fig 9. Calculated life ratio for a constant stress amplitude at half life

3.3. Main crack initiation sites

Several tests were stopped at different fraction of life in order to study the crack initiation using the replica technique (figures 10 and 11). These interrupted tests have shown that crack initiation stage covers the major part of the life when number of cycles to failure is superior to few ten thousands cycles. So, the crack initiation stage controls the number of cycles to failure, therefore we systematically observed the crack initiation sites after the test. Three main crack initiation sites were observed (figure 12) :

- Non Metallic Inclusion (NMI)
- Prior austenitic grain boundary
- Lath boundary

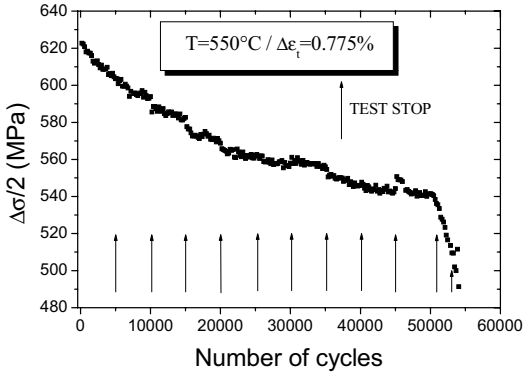

Fig 10. Interrupted test performed at 550°C

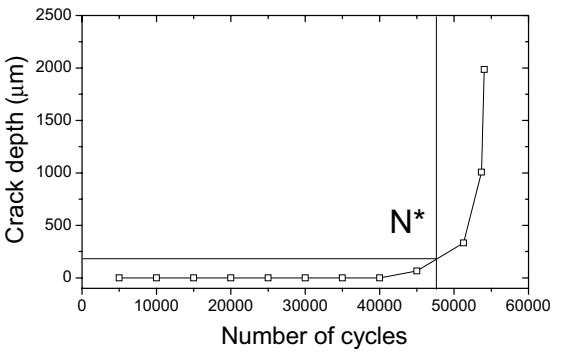

Fig. 11. Crack depth according to the number of cycles (same experimental conditions as fig. 10)

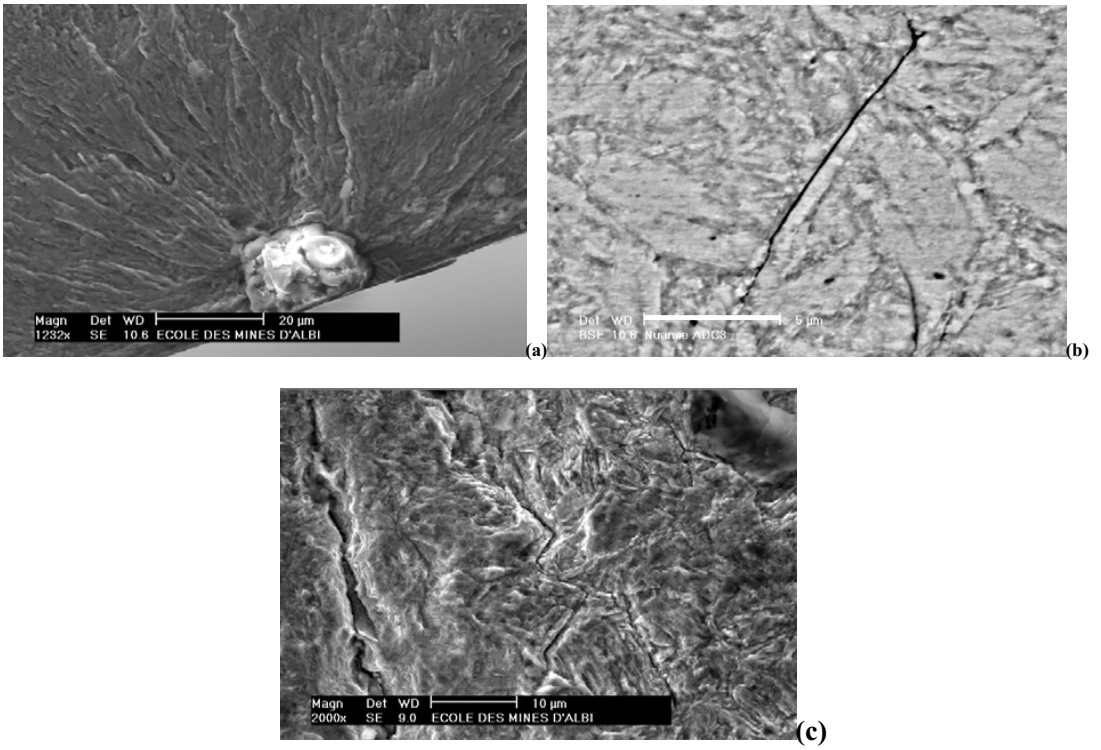

Fig. 12. Main fatigue crack initiation sites (a) non metallic inclusion (b) lath boundary (c) prior austenitic grain boundary

Figure 13 presents the fraction of dominant crack initiation site versus the temperature where ρ', ρ'', ρ''' are respectively the proportion of crack initiation on NMI, prior austenitic grain boundary and lath boundary. Crack initiation on NMI was mainly observed at low temperatures (200°C-400°C). Globular silicates and aluminium oxides inclusions were mainly found on the rupture surface. The occurrence of crack initiation on inclusions at low temperatures is strongly associated to the probability to find a NMI near the specimen surface. It was possible to calculate the NMI size which leads to the specimen rupture for a given rupture probability [29,30]. Between 200°C and 400°C, the lower NMI size observed on the surface after rupture is 7.5µm and experimental probability of rupture due to NMI is 46.6% for 30 specimens observed. For the same probability, the NMI critical size calculation gave a range between 6µm and 10µm depending on NMI distribution heterogeneity [2].

Figure 13 shows that crack initiation mechanisms is strongly dependant on testing temperature : competition between lath boundary and NMI between 200°C and 400°C and prior austenitic grain boundary between 500°C and 600°C. Crack initiation on prior austenitic grain boundary was observed for the highest temperatures (500°C-600°C). This mechanism seems to be associated to a local preferential oxidation. Oxidation mechanisms described by N.Tsujii et al. [31] and [32,33] seem to have an important role on crack initiation. Two tests under controlled atmosphere were performed at 550°C at the University of Braunschweig. Both tests have revealed a crack initiation on lath boundary exactly as it was observed at lower temperatures. Consequently, crack initiation is also dependent on environment. However, more fatigue tests are necessary to quantify the parts of life decrease due to the loss of mechanical properties and due to the surface effect. This last research goal certainly represents one of the most interesting outlook of this study.

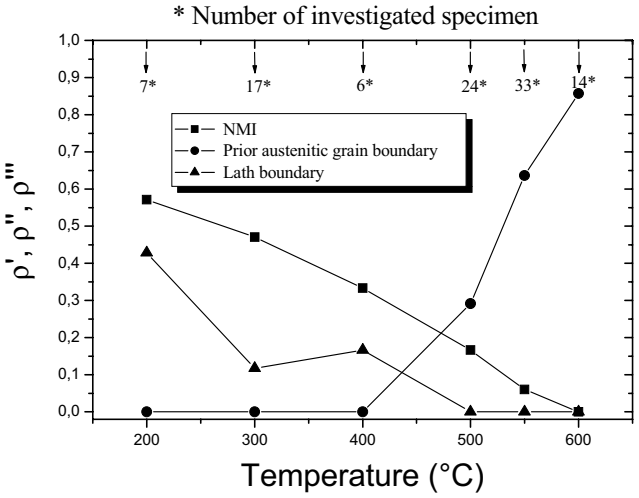

Fig 13. Fraction of dominant crack initiation site according to the testing temperature

4. Conclusion

Continuous cyclic softening has been observed on a tempered martensitic tool steel. For a critical strain amplitude which depends on temperature and initial hardness, it leads to a strong effect that should be taken into account in the definition of a tool geometry. This typical behaviour is associated to dislocations rearrangement and carbides coalescence during cycling. TEM observations and XRD have been performed to quantify microstructure relevant parameters variations during a tempering treatment and a fatigue test.

Influences of temperature and hardness on fatigue life were also studied. Both influences are limited when observed through a Manson-Coffin diagram. Conversely, increasing testing temperature or decreasing hardness leads to a strong reduction of life when results are plotted in a Basquin diagram.

Observations of surface rupture revealed 3 main mechanisms of crack initiation strongly dependent on testing temperature and environment :

- Non Metallic Inclusion (200°C-400°C)
- Lath boundary (200°C-400°C)
- Prior austenitic grain boundary (500°C-600°C)

Acknowledgements

Authors gratefully acknowledge AUBERT & DUVAL (A&D) company for supplying the steels and for the financial support, the University of Braunschweig for the realisation of fatigue tests in inert gas and Professor T.Ungár from the Eötvos University of Budapest for the x-ray diffraction experiments and for the invaluable help in the peak profile analysis.

References

[1] G.A. Roberts and R.A. Cary. *Tool steels*, American Society for Metals (Eds.), Metals park, Ohio, USA, 4th edition, 1980.

[2] D. Delagnes. Ph.D. *Thesis*, Ecole Nationale Supérieure des Mines de Paris, 1998.

[3] N. Mebarki, D. Delagnes, P. Lamesle, F. Delmas and C. Levaillant. *Mater. Sci. Eng*. 2004;**A 387-389**:171.

[4] Z. Zhang, D. Delagnes and G. Bernhart. *Inter. J. of Fat*. 2002;**24**:635.

[5] V. Velay, G. Bernhart, D. Delagnes and L. Penazzi , *Fat. Frac. Eng. Mater. Struct* 2005;**28**:1009.

[6] T. Ungár and A. Borbély. *Appl.Phys.Lett*. 1996;**69**:3173.

[7] Á. Révész, T. Ungár, A. Borbély, and J.Lendvai. *Nanostr. Mater*. 1996;**7**:779.

[8] J. Gubicza, J. Szépvölgyi, I. Mohai, L.Zsoldos and T.Ungár. *Mater. Sci. Eng. A* 2000;**280**:263.

[9] G. Dour, M. Dargusch, C. Davidson, A. Nef, D. St John and A. Dahle (Eds.) *Conference Light Metals Technology*. Brisbane (Australia), 2003, 155.

[10] R.A. Fournelle, E.A. Grey, and M.E. Fine. *Metall. Trans*. 1976;**7A**:669.

[11] K. Kanazawa, K. Yamaguchi and K. Kobayashi. *Mater. Sci. Eng*. 1979;**40**:89.

[12] J.B. Vogt, G.Degallaix and J. Foct. *J. Fatigue Frac. Eng. Mater. Struct*. 1988;**11**:435.

[13] J.C. Earthman, G. Eggeler and B. Ilschner. *Mater. Sci. Eng. A* 1989;**110**:103.

[14] S.R. Mediratta, V. Ramaswamy, V. Singh and R.Rao. *Steel Research* 1990;**61**:325.

[15] H.J. Christ, C. Sommer, H. Mughrabi, A.P. Voskamp, J.M. Beswick and F. Hengerer. *J. Fatigue Frac. Eng. Mater. Struct*. 1992;**15**:855.

[16] H. Chai and Q. Fan. Fatigue 93, *5th international conference on fatigue and fatigue thresholds*, Montreal (Canada), 1993, 195.

[17] S. Sankaran, V. Subramanya Sarma and K.A. Padmanabhan. *Mater. Sci. Eng. A* 2003;**345**:328.

[18] B. Fournier, M. Sauzay, C. Caës, M. Noblecourt and M. Mottot. *Mater. Sci. Eng. A* 2006;**437**:183.

[19] Z.G. Wang, K. Rahka, P. Nenonen and C. Laird. *Acta Metall*. 1985;**33**:2129.

[20] A. Joarder, N.S. Cheruvu and D.S.Sarma. *Mat. Charact*. 1992;**28**:121.

[21] H.J. Chang, C.H. Tsai and J.J. Kai. *Int. J. Pres. Ves. & Piping*, 1994;**59**:31.

[22] J. Pešička, R. Kužel, A. Dronhofer and G. Eggeler. *Acta Mater*. 2003;**51**:4847.

[23] G. Eggeler. *Acta Metall*. 1989;**37**:3225.

[24] J. Pešička, A. Aghani, Ch. Somsen, A. Hartmaier and G. Eggeler. *Scripta mater*. 2010;**62**:353.

[25] Z. Zhang, D. Delagnes and G. Bernhart. *Mater. Sci. Eng. A* 2004;**380**:222.

[26] T. Ungár, S. Ott, P.G. Sanders, A. Borbély and J.R. Weertman. *Acta mater*., 1998;**46**:3693.

[27] T. Ungár, J. Gubicza, G. Ribárik and A.Borbély. *J.Appl. Cryst*., 2001;**34**:298.

[28] N. Mebarki, P. Lamesle, D. Delagnes, F. Delmas, C.Levaillant and J.Bergström et al. (Eds.). *6th International Tooling Conference, The Use of Tool Steels : Experience and Research*, Karlstad University (Eds.) Sweden, 2002, 617.

[29] A. Pineau. *High Temperature materials for power engineering*, E. Bachelet (Eds.), 1990, 913.

[30] A. De Bussac and J.C. Lautridou. *La revue scientifique Snecma*, 1994, 63.

[31] N.Tsujii, G. Abe, K. Fukaura and H. Sunada. *ISIJ International* 1995;**35**:920.

[32] A. Oudin, P. Lamesle, L. Penazzi, S. Le Roux and F.Rézaï-Aria. *European structural integrity society* **29** (2002) 195.

[33] B. Miquel, S. Jean, S. Le Roux, P. Lamesle and F.Réraï-Aria. *European structural integrity society* **29** (2002) 183.